Journal of Chromatography, 316 (1984) 311–332
Elsevier Science Publishers B.V., Amsterdam — Printed in The Netherlands

CHROMSYMP. 449

THEORETICAL MODELS FOR SIZE-EXCLUSION CHROMATOGRAPHY AND CALCULATION OF PORE SIZE DISTRIBUTION FROM SIZE-EXCLUSION CHROMATOGRAPHY DATA

JOHN H. KNOX* and HUGH P. SCOTT*
Department of Chemistry, University of Edinburgh, West Mains Road, Edinburgh EH9 3JJ (U.K.)

SUMMARY

Size-exclusion chromatography (SEC) calibration curves are calculated using a range of models starting from those with simple, uniform pore geometry and culminating in a computer-assembled model, consisting of random-size touching spheres. This final model provides an excellent correlation between experimental data obtained with Hypersil and theoretical prediction with virtually no adjustable parameters. Very good correlation is also obtained using the uniform-size random-sphere model of Van Krefeld and Van den Hoed. It is shown that SEC calibration curves can also be predicted with remarkable accuracy from mercury porosimetry data on the assumption that the matrix consists of an assembly of cylindrical channels having the same pore-volume distribution as that provided by mercury porosimetry. A simple mathematical inversion of this procedure enables the pore size distribution to be precisely determined from any SEC calibration curve. A serious error in previous procedures is noted and corrected.

INTRODUCTION

In chromatography a solute is said to be "excluded" if it travels along the column faster than eluent. Exclusion can arise for several reasons. If one component of an eluent is more strongly retained than solute, then the solute will be unable to displace eluent from the surface layer and so it will be excluded from that layer[1]; if the solute is charged and has the same charge as the particles of packing, it will have difficulty entering the particles due to the Donnan potential at the surface[2]; if solute molecules have dimensions commensurate with the pore dimensions, they will be sterically excluded from part of the pore volume. Only the last of these reasons for exclusion is widely used as a basis for separation in the technique known as size-exclusion chromatography (SEC)[3], gel-filtration (GF)[4] or gel-permeation chromatography (GPC)[5].

Theories to explain size exclusion have been based upon differing rates of dif-

* Present address, Department of Pharmacy, Heriot-Watt University, Grassmarket, Edinburgh, U.K.

0021-9673/84/$03.00

fusion of molecules of different size[6], differential flow profiles in channels of the packing[7,8] and upon steric effects[9,10]. The majority of chromatographers now agree[3] that size separation of molecules can be fully explained on the purely steric basis that large molecules can only partially permeate the pore volume of the support. According to this view, small molecules (such as those of eluent) fully permeate the pores of the support material and are eluted in the void volume, V_m; large molecules which cannot enter any of the pores are totally excluded and are eluted in the extra-particle volume, V_o; molecules of intermediate size are eluted between V_o and V_m. The degree of permeation of such molecules into the pore volume of the particles, V_p, is denoted by K, and termed the "exclusion coefficient". K is related to the elution volume, V_R, of any solute by eqn. 1. K can have any value between 0 and 1.

$$V_R = V_o + KV_p \tag{1}$$

The pore volume is related to V_m and V_o by eqn. 2.

$$V_m = V_o + V_p \tag{2}$$

The relationship of retention volume or exclusion coefficient to molecular weight for any packing material is normally displayed as a plot of log MW against V_R or K, and is called an exclusion curve or SEC calibration curve. Typical examples are shown in Fig. 1.

Since molecular weight is directly related to molecular radius for any polymer

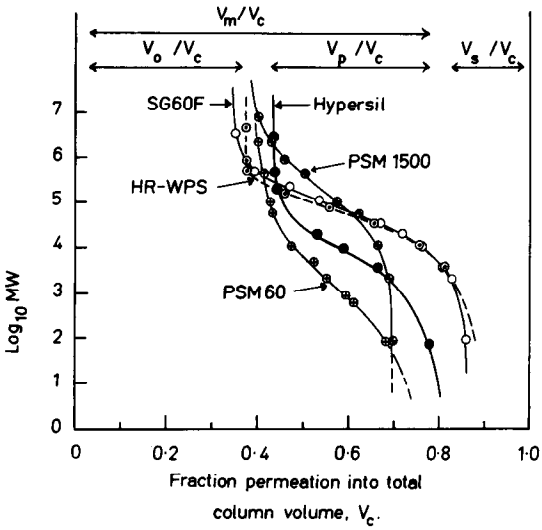

Fig. 1. SEC calibration curves for polystyrene standards eluted from various silica gels with "uniform" pore size distributions (for further details see original reference). Hypersil[11] = commercial sample from Shandon Southern Products, Runcorn, U.K.; SG60F[11] = Experimental SEC material, prepared by AERE, Harwell, U.K.; PSG60 and PSG1500[3] = SEC materials, prepared by Du Pont, Wilmington, DE U.S.A.; HR-WPS = experimental wide-pore, high-porosity silica gel, prepared by H. Ritchie, Department of Chemistry, University of Edinburgh. [Note: the values of V_m and V_o for PSG60 and PSG1500 are estimated from data given (ref. 3)].

in a given solvent, SEC calibration curves can easily be adapted to show the dependence of V_R or K upon molecular radius. Such curves can then be compared directly with theoretically predicted exclusion curves.

THEORETICAL EXCLUSION CURVES FOR SIMPLE PORE GEOMETRIES

We assume in what follows that the exclusion coefficient, K, of a solute depends only upon the size and shape of the solute molecules and upon the size and shape of the pores in the column packing material. We also assume that the molecules of solute can be considered rigid, and that band spreading arises only from kinetic effects and the polydispersity of the sample, as shown by Knox and McLennan[11], amongst others.

The way in which K is expected to depend upon molecular size can be illustrated by a simple example. The solute molecule is taken as a "hard sphere" of radius r and the pore is an infinite cylinder of radius R. Since the centre of mass of the molecule cannot approach closer than a distance r from the wall of the pore, the part of the pore volume accessible to the centre of mass is a cylinder of radius $(R-r)$. Thus the exclusion coefficient, which is equal to the fraction of the total pore volume accessible to the molecule, is

$$K = \left(1 - \frac{r}{R}\right)^2; \qquad \left(\frac{r}{R}\right) < 1 \tag{3a}$$

$$K = 0; \qquad \left(\frac{r}{R}\right) > 1 \tag{3b}$$

The above example is a special case of the general equation for spherical molecules, which gives K as the ratio of the volume of pores accessible to the centre of mass of the molecules (V_a) to the total volume of the pores (V_p)

$$K = \frac{V_a}{V_p} \tag{4}$$

This simple hypothesis ignores problems of access to pores which may have restricted entrances. However, we may assume that swollen polymer molecules, even if apparently spherical for a high proportion of time, will be able by random processes to achieve configurations suitable for squeezing through narrow pores, even if their mean time of residence in such pores is very small. Thus, the problem is one of mass transfer, not of thermodynamic equilibrium.

For non-spherical molecules the problem of calculating K is complex, since the distance of closest approach of the centre of mass to the pore wall by, say, a rod-like molecule depends upon its orientation relative to the wall. The problem is soluble by statistical methods and has been treated by Giddings *et al.*[9]. V_a and V_p can now be regarded as volumes in configuration phase space.

In this paper we restrict ourselves to essentially spherical molecules which will be assumed to be rigid. This applies with reasonable accuracy to many synthetic

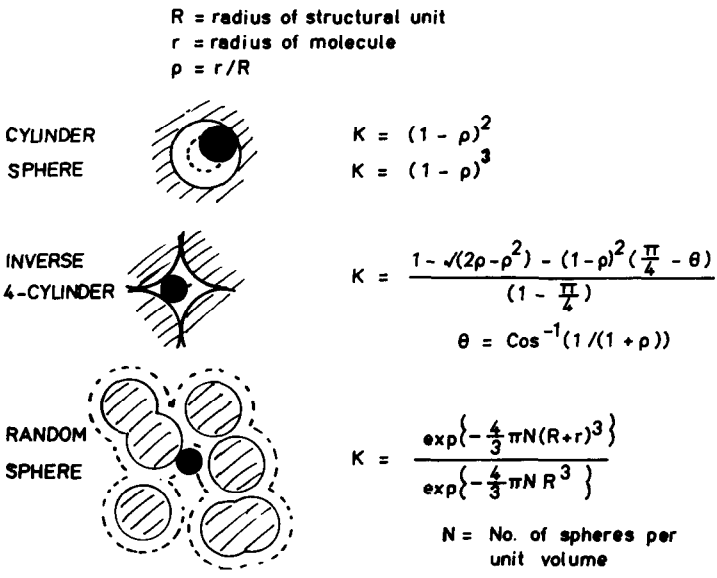

Fig. 2. Illustration of exclusion from pores of simple and random sphere[12] model with appropriate equations for exclusion coefficient K.

polymers in good solvents whose random chains on the average fill a roughly spherical space.

Exclusion curves for spherical molecules are readily calculated for simple pore geometries[10]. Equations for a number of such cases, including the cylindrical pore, are given in Fig. 2. The pore of the "inverse cylinder" model consists of the space between touching cylinders (three or four) and that of the "regular sphere matrix" (see below) is the space between touching spheres positioned at the corners of a cube. The random sphere model[12,13], also included in Fig. 2, is discussed below.

Exclusion curves for the simple geometrical models are given in Fig. 3, where K is shown as a function of the Naperian logarithm of the molecular radius ratio, r/R.

All curves in Fig. 3 have broadly similar shapes. The following points may be noted. (1) For small molecules the curves descend very steeply, showing a decreasing change in K as the size falls to zero. (2) For molecules of intermediate size there is a region where K depends more or less linearly on ln (r/R). This covers a roughly five-fold range of (r/R). (3) For large molecules near the exclusion limit there is generally a slight upward curvature of the exclusion curve which is most noticeable for the "regular sphere matrix". In general, experimental curves show much more gradual transitions to complete exclusion, a somewhat steeper gradient in the intermediate region, and a less pronounced descent at K approaching unity.

It is noted that the curves for the inverse cylinders and simple cubic matrix cut the vertical axis (the point corresponding to complete exclusion) below the origin [corresponding to $(r/R) = 1$]. This is an artefact of the definition of R as the radius of the typical element rather than as the radius of the largest sphere, R', which can be accommodated. The ratios R'/R for the different cases are 0.732 for regular sphere matrix, 0.414 for the inverse 4-cylinder, and 0.153 for the inverse 3-cylinder. Re-

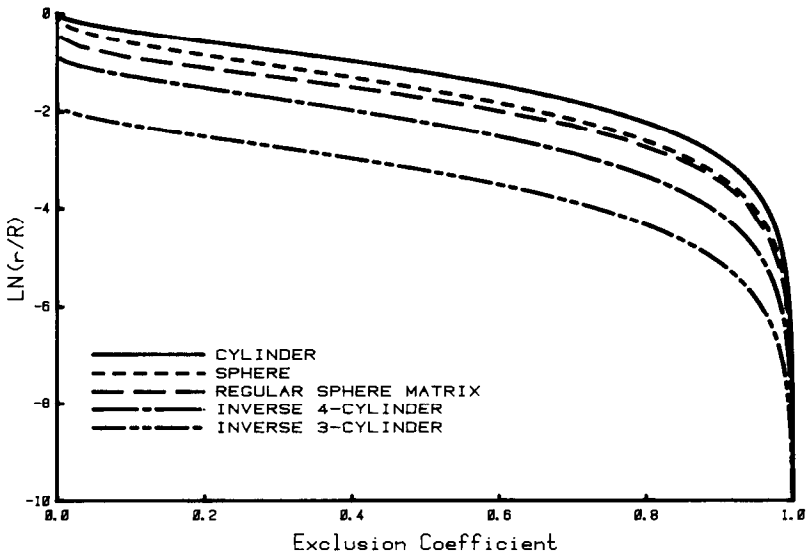

Fig. 3. Exclusion curves for simple models. r = Radius of polymer molecule; R = radius of structural unit (see Fig. 2 and text).

plotting the curves in terms of (r/R') brings them very close together, as shown in Fig. 4.

In order to compare experimental data obtained by elution of a particular solute from a particular matrix with theoretical predictions based upon a model, it is necessary to know the relationship between molecular radius and molecular weight

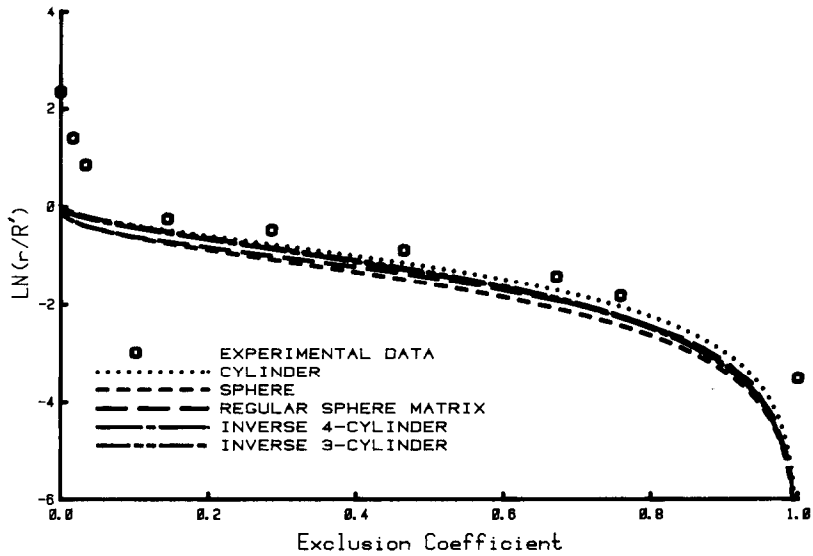

Fig. 4. Exclusion curves for simple models. r = Radius of polymer molecule; R' = radius of largest sphere which can be accommodated by model pore. Experimental data is for Hypersil from Fig. 1.

for the solute, along with some broad geometrical properties of the matrix, such as mean pore diameter and porosity.

The effective radius of a sphere, r, is related to its radius of gyration, r_g, by eqn. 5.

$$r = 0.886\, r_g \tag{5}$$

and for random chain polymers r_g is given by eqn. 6.

$$r_g = aM^b \tag{6}$$

where M is the relative molecular weight. Use of published values of the constants a and b for polystyrenes[3,13] gives eqn. 7 for the effective sphere radius r of polystyrenes:

$$r/\text{Å} = 0.123M^{0.588} \tag{7}$$

In order to obtain appropriate characteristics of the matrix, in this case Hypersil, we assume that the material is made up of random-sized colloidal spheres. The specific surface area is about 200 $m^2\ g^{-1}$, and the density of silica is 2.20 g cm^{-3}. The mean colloidal sphere radius, R, is then 68 Å. The mean pore radius, R', will be different from R, but in view of the complex geometry of the space in the material no simple estimate of r/R' is possible. Accordingly, a value of 68 Å is used for both R and R'.

Fig. 4 compares the theoretical curves for the simple models, plotted on the basis of ln (r/R') against K, with the experimental data for Hypersil. The fit is seen to be surprisingly good in view of the approximation $R' = R$ in Hypersil. Closer examination shows that the fit is good in the central region both as regards position and gradient but poor at the extremes. At both high and low MW the experimental data lie above the theoretical curves. As seen later the discrepancies are explained by noting that even small molecules, such as benzene, have finite size and are partially excluded from the pore volume and that real materials have a range of pore sizes.

The theoretical exclusion curves presented in Figs. 3 and 4 do, however, emphasise that even for uniform pores there is no sudden transition from total permeation to total exclusion, as has sometimes been assumed[14], and that the pore shape has little effect on the theoretical curves.

EXCLUSION CURVES FOR RANDOM PORE MODELS

The pore models so far described have been of regular geometry, and each model consists of pores of a single uniform size. Clearly no such model can accurately represent real packing materials for SEC. While the nanometre-sized units which make up the particles of such materials may well be spherical, neither they nor the pores which they define will be of a uniform size, nor will they be positioned in a regular array.

One model which overcomes some of these shortcomings is the random-sphere model[12] used by Van Krefeld and Van den Hoed[13]. This model is generated by growing spheres of equal size centred on random points in space. The spheres are allowed to overlap as required. The void volume of such a model is simply calculated

by statistical methods and the exclusion curve is calculated by first of all setting the porosity at some starting value (for example the porosity of the experimental material) and then calculating porosities with increased sphere sizes. The starting sphere diameter is taken as R and the subsequent sphere diameters represent $(R+r)$. K is then found as the ratio of the porosity at $(R+r)$ to the porosity at R. Van Krefeld and Van den Hoed[13], using this model, obtained more or less perfect agreement between their predictions and data obtained with Porasil.

This model, however, may be criticised on the grounds that it is still composed of uniform-sized spheres and that their overlap may not properly model the real situation where colloidal spheres of random size are simply agglomerated and only make contact over an extremely small area.

Our objective was to develop and test a somewhat more realistic model. The radii of the spherical units were accordingly chosen randomly from a Gaussian distribution and, in assembling the model, these spheres were not allowed to overlap. In this way, the proportion of the pore volume in the cusp-shaped regions between touching spheres would be maximized, while the random distribution of unit sizes would provide a somewhat wider pore-size range than possible with any uniform sphere model. Since statistical methods are no longer applicable, computer calculation was used both to assemble the model and to evaluate its properties.

Computer simulations of random packings of spheres have been carried out by various groups. Adams and Matheson[15] considered packing spheres in a centrosymmetric gravitational field. Visscher and Bolsterli[16] assumed a uni-directional field; their method is similar to packing ball-bearings into a jar. Although the model developed below has features in common with both, it was developed quite independently, and differs significantly in the range of sphere radii considered.

Two models were developed. The first consisted of random touching circles, and the second of random touching spheres. In each case it is the space between these units which is under consideration. The "touching sphere" model is the three-dimensional analogue of the "touching circle" model which is, of course, equivalent to a "touching cylinder" model.

Flow diagrams for the "touching circle" and "touching sphere" models are shown in Fig. 5. For both models, the radii are produced from a pseudorandom normal distribution with a mean of one unit. In the "circles" model standard deviations of 0.1 and 0.3 units were used, in the "spheres" model the standard deviation was 0.1 unit.

The first step in the "circles" program is to define a base upon which future circles will rest. This base consists of a line of touching circles of randomly chosen radii, but with their centres on the x-axis. The final circle on this base becomes the starting circle for positioning the first circle of the next row.

All subsequent circles are positioned to touch the previously positioned circle, and (if possible) the nearest circle to it in a specified direction. The position of the centre of the new circle is at the third vertex of a triangle whose other vertices are at the centres of these two circles. The length of the sides are defined by the radii of the two starting circles and the new circle.

As shown in Fig. 6A, there are two possible positions for the centre of the new circle, as defined by the above algorithm. If the new circle impinges on any other circle as a result of the first solution, the alternative solution is examined. If neither

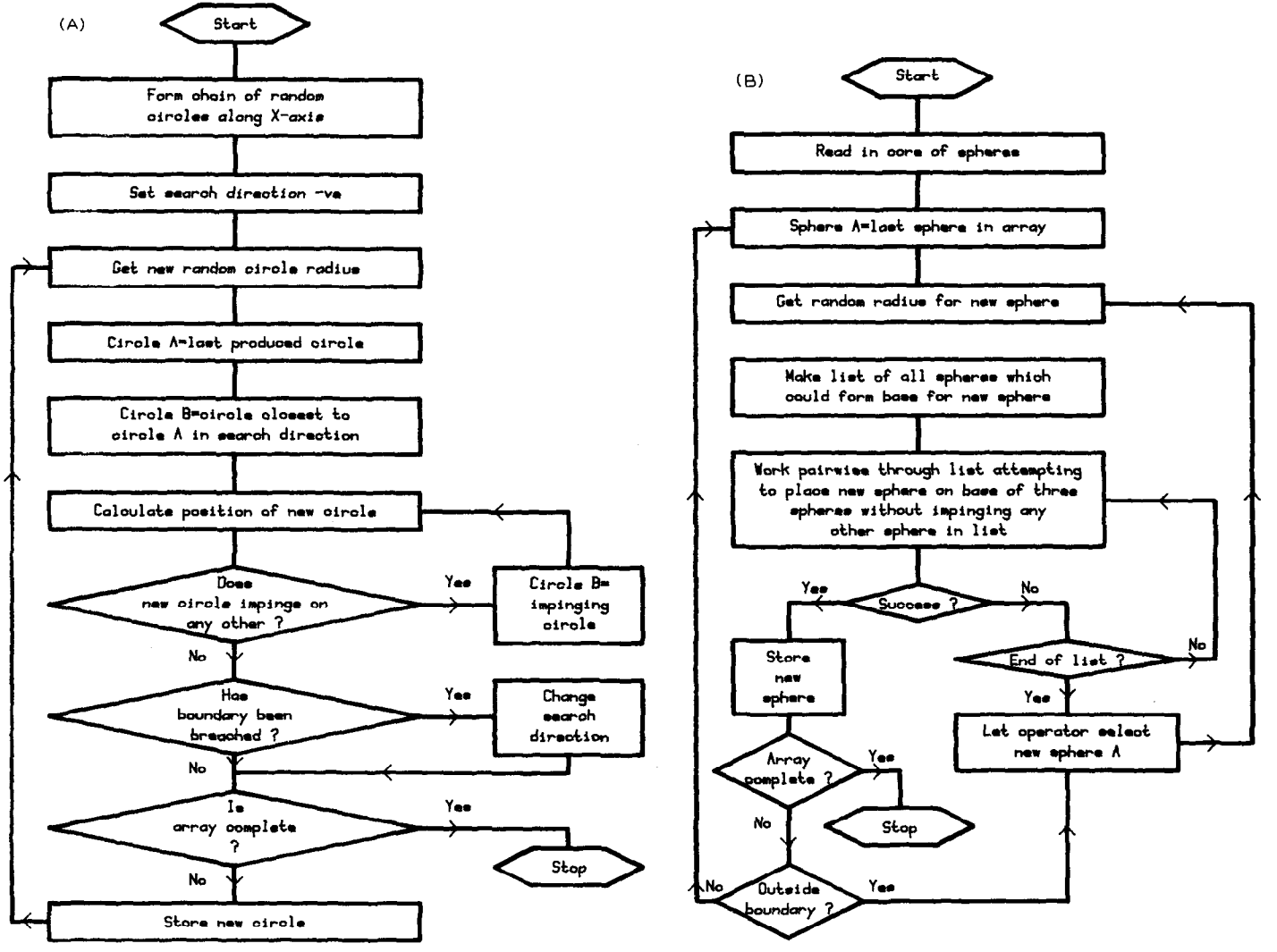

Fig. 5. Flow diagrams for computer assembly of models of (A) touching circles, (B) touching spheres.

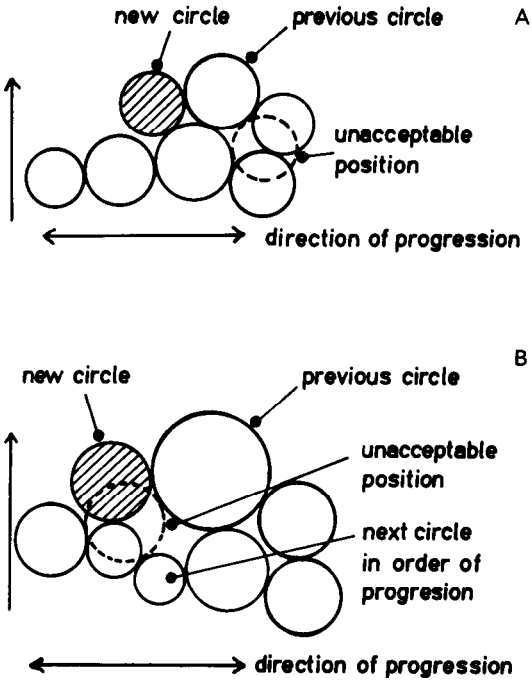

Fig. 6. Illustration of geometrical constructions for assembling model of touching circles. (A) Case where nearest-circle to last-added-circle provides position of new-circle. (B) Case where circle other than nearest-circle must be used.

solution is successful, as shown in Fig. 6B, an alternative choice of the second starting circle is required.

This process is repeated with appropriate reversal of the direction of search after each row is completed. The program terminates when the array is about as tall as it is long.

In the "sphere" model the base was replaced by a core of five spheres with radii close to unity. Each subsequent sphere requires three spheres to rest on, and the position of the centre of the new sphere is the fourth vertex of a tetrahedron. The other three vertices are the three spheres on which the new sphere rests, and the remaining edges have lengths defined by the sum of the new sphere radius and the radii of these "base" spheres. The solution to the tetrahedron problem is given by Scott[17].

Again two possible solutions are available, and both positions for the centre of the new sphere are tested to see whether the new sphere impinges on any other sphere. If neither position is satisfactory then other base spheres are used until a permissible position for the new sphere is found.

In building the "sphere" model it sometimes happened that no satisfactory solution could be found, or that a "string" of spheres was produced which reached the intended boundary of the array without filling the space around the string. In these cases a completely fresh starting sphere was used, rather than the last sphere added. This required operator intervention, but we do not believe that this significantly corrupted the randomness of the model.

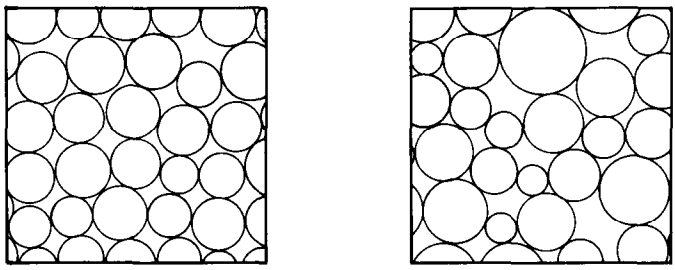

Fig. 7. Computer-assembled arrays of random-sized touching circles. Standard deviation of circle radii = 0.1 and 0.3 units, mean circle radius = 1 unit.

The completed arrays of circles contained about 100 circles. A central region only was used for the calculation of exclusion curves in order to avoid edge effects and the effect of the base line of circles. The portions of the arrays used for further calculations are shown in Fig. 7. The porosities of these arrays are 18.7% and 21.1%, respectively.

The completed array of spheres contained about 1800 spheres, from which a central portion containing about 1600 spheres was used for exclusion coefficient calculations. Two sections through the array are shown in Fig. 8. The variation in circle size and the fact that they do not touch arises, of course, from Fig. 8 being a section through the array of spheres: about half of the circles represent spheres with centres above the plane of the figure and the remainder below. The porosity of the array was calculated (see below) to be 43%, which is close to the experimental value of 37–45% for arrays of randomly packed spheres but well below 61%, the porosity of Hypersil. A full listing of the radii and the coordinates of the centres of the spheres may be obtained from the authors.

To calculate the porosity of the arrays of circles, and to derive the exclusion curves, each array was examined point by point. The fractional void volume or porosity was then given by the ratio of the number of test points found to be outside the circles to the total number of test points. The distance between neighbouring test points was as small as practicable within the constraints of available computer time

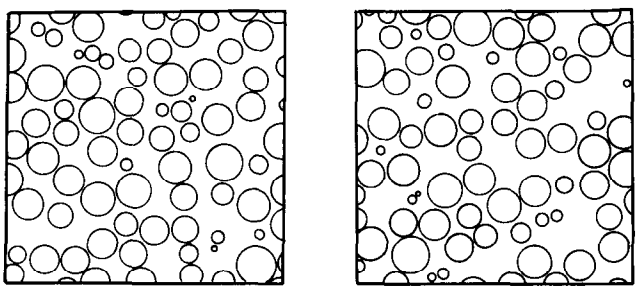

Fig. 8. Sections through array of random-sized touching spheres having standard deviation of sphere radius = 0.1 unit, and mean sphere radius = 1 unit.

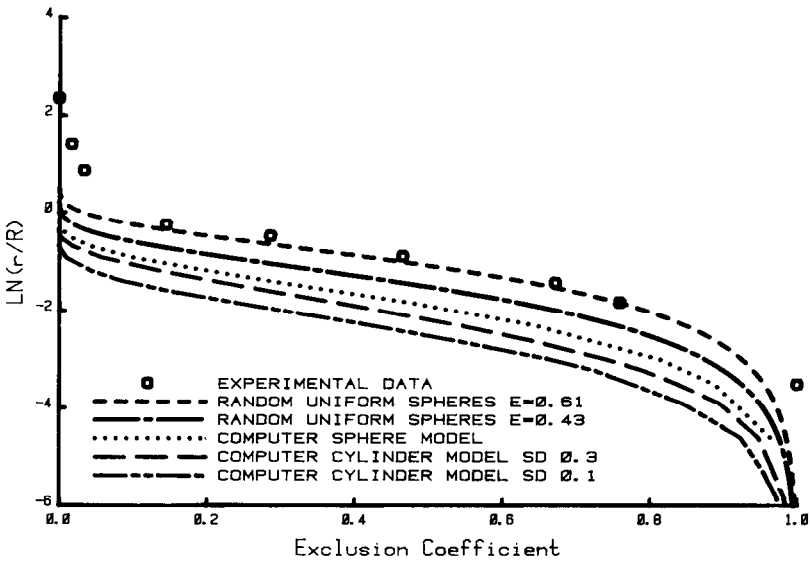

Fig. 9. Exclusion curves for complex models (for details see text). Experimental data for Hypersil from Fig. 1.

(typically 10 points per linear unit). Exclusion curves for the "circle" models were calculated by increasing the radius of each circle by the molecular radius under consideration and re-calculating the void volume by the above method.

For the array of spheres a more efficient method for obtaining the exclusion curve was required. For each test point in the unoccupied space the shortest distance to a sphere surface was calculated. Molecules with radii greater than this distance were then "excluded" at this point. In this way each test-point needed to be considered only once. The results are shown in Fig. 9 along with the experimental data for Hypersil positioned on the ln (r/R) axis, using the calculated mean sphere radius R = 68 Å.

Fig. 9 also includes curves calculated for the random sphere model of Van Krefeld[13]. For this model

$$\ln \psi_{(R+r)} = \frac{-4}{3} \pi N(R + r)^3 \tag{8a}$$

where N is the number of spheres per unit volume, and

$$K = \psi_{(R+r)}/\psi_R \tag{8b}$$

Two curves are shown, one based on ψ_R = 0.43 the porosity of the model of random touching spheres, and the second based on ψ_R = 0.61, the experimentally measured porosity of Hypersil[11].

The theoretical curves of Fig. 9 all have the same general shape. The models based on circles or spheres of a range of size, that is the models developed by us, show a steeper central portion than does the uniform-size random sphere model of Van Krefeld: it is also noticeable that the circle model with the wide range of circle sizes (S.D. = 0.3) gives a slightly steeper curve than the model with the narrower range (S.D. = 0.1).

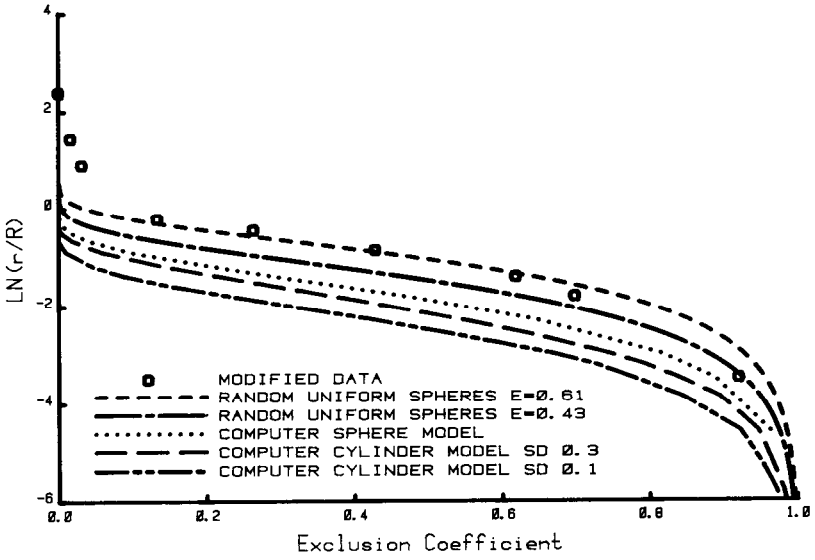

Fig. 10. As for Fig. 9, but experimental data adjusted to give K (benzene) = 0.92.

The two curves for the Van Krefeld model show the effect of adjusting the porosity of the model. When the porosity is increased, the mean pore size, R', increases relative to the radius of the spherical units R, and therefore the exclusion curve when plotted on the basis of r/R is higher the larger the porosity.

The comparison of experimental and calculated curves shows the excellent agreement between experiment and the Van Krefeld model with the correct porosity, but the same divergencies are noted as when using simple geometric models (see Fig. 4). It might be expected that an upward adjustment of the porosities of our models would likewise raise the curves, bringing them into better agreement, but first we address the problem of the divergence between experiment and theory at the low-molecular-weight end of the scale. As K approaches unity the theoretical curves all turn sharply downwards while the experimental curve is rather flat. The reason for this is primarily that even a small molecule, such as benzene, has a finite size and, when attempting correlation with theoretical calculations, it must be assigned an appropriate value of K less than unity.

Using the random touching sphere model in conjunction with the known molecular radius of benzene and the unit size in Hypersil, K for benzene is calculated to be 0.92. Thus, the experimental curve should be compressed laterally so that the last point appears with this K value. Fig. 10 shows the data replotted in this way. It is now noted that as far as gradient is concerned, the random-size touching sphere and circle models provide a better fit than the uniform-size random sphere model. This illustrates the importance of building into the model an adequate pore size distribution by using building units with a range of sizes.

Two requirements must evidently be met if a model is to provide quantitative agreement with experiment. (1) The porosity of the model must be the same as that of the experimental material. (2) The model must provide an adequate range of pore size by employing building units of a range of sizes. It appears that a standard de-

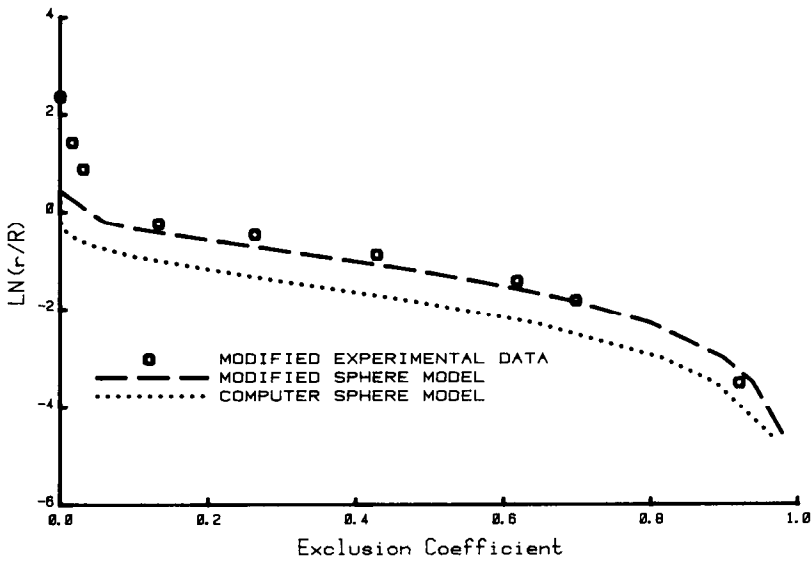

Fig. 11. Effect of increasing porosity on exclusion curve for random-size sphere model. "Computer sphere model" has porosity of 43%; "modified sphere model" has porosity increased to 56% by randomly removing spheres from the array. Experimental data for Hypersil, plotted as in Fig. 10.

viation of between 0.1 and 0.3 meets this requirement for a material like Hypersil.

Our present model comprising random size touching spheres is not as readily amenable to alteration of porosity as in the Van Krefeld model. We have therefore adopted the method of "removing" spheres at random in order to produce an appropriate porosity and also a wider range of pore sizes. In this way, the porosity has been increased from 43 to 56%, fairly close to the 61% of Hypersil. Fig. 11 shows that this procedure results in almost perfect agreement between theory and experiment, except at the highest molecular radii.

PREDICTION OF EXCLUSION CURVES FROM POROSIMETRY DATA: SIMPLE MODELS WITH A RANGE OF UNIT SIZE

All curves for the random sphere or circle models show a better fit to experiment than do the simple geometric models. However, the improvement is not as decisive as might have been expected. Indeed, the rather slight improvement in going from the simplest model of a uniform cylindrical pore to the most complex model of random size touching spheres is something of a disappointment. The question then arises as to whether adaptation of the simple models to include a range of pore sizes might not be a simpler and possibly more useful approach of prediction of exclusion curves.

Mercury porosimetry provides a means of determining experimentally the pore size distribution of any material. The results are interpreted on the basis of an assumption that the pores of the material are cylindrical[18] and therefore that the material consists of a structure containing a range of cylindrical pores. If this model were realistic then an exclusion curve should be readily calculable from the pore size

distribution. It is easily shown (see Appendix) that if f(R) is the volume fraction of pores of radius R, then the exclusion coefficient for a molecule of radius, r, is given by eqn. 9.

$$K = \sum_{R=r}^{R=\infty} \mathrm{f}(R)\left(1 - \frac{r}{R}\right)^2 \tag{9}$$

For a continuous distribution function, where f'(R)dR represents the fraction of pore volume within a range R to $R + \mathrm{d}R$, K is given by eqn. 10.

$$K = \int_{R=r}^{R=\infty} \mathrm{f}'(R)\left(1 - \frac{r}{R}\right)^2 \mathrm{d}R \tag{10}$$

The full pore-size distribution curve (cumulative) for 5 μm Hypersil particles is shown in Fig. 12. There is a fairly clear distinction between the relatively wide pores which occur between particles (interparticle pores) and the much smaller pores which occur within the particles (intraparticle pores). However, in regard to the exclusion phenomenon there is no distinction between the two types of pores, and exclusion of suitable sized molecules will occur from both inter- and intra-particle pores. Small enough molecules will penetrate the smallest intraparticle pores, while sufficiently large molecules may be partially excluded from some of the interparticle pores. In order to make use of eqns. 9 and 10 it is therefore important to decide upon the maximum pore diamter which need be included in any theoretical treatment; that is one must decide upon a suitable radius at which the pore size distribution curve can be truncated without introducing significant error in the calculated exclusion curve. Because molecules are partially excluded even from pores which are considerably larger than the diamter of the molecule itself, it is clear that this truncation must

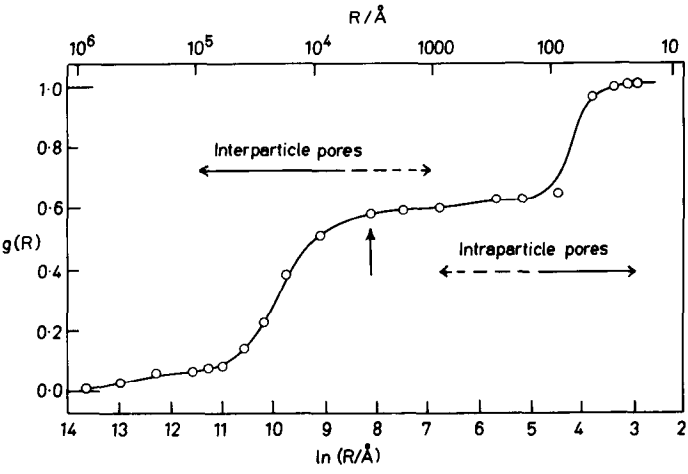

Fig. 12. Complete pore-size distribution curve for 5 μm Hypersil obtained by Mercury porosimetry (Coulter Instruments). Arrow indicates cut-off point for calculations.

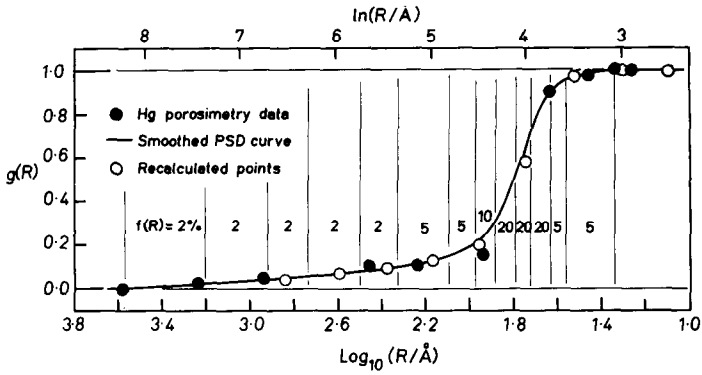

Fig. 13. Pore-size distribution curve used for calculations. (●) Experimental data; full line from smoothed data used for calculation; segments used for f(R) are indicated by % of total pore volume; (○) calculated pore size distribution (see text).

be at a value of R which is many times greater than the radius of the largest molecule of interest. Roughly speaking, an appropriate value will be not less than ten times the maximum molecular diameter unless the fraction of large pores is itself very small. By truncating the pore-size distribution curve at a pore radius well above that of the largest molecule it will be found that the K value for this molecule will not be zero but will have some positive value K_0. Since it is normal to assign a K value of zero to such a molecule, an adjustment to the calculated K values is required. This is given by the simple eqn. 11.

$$K_{new} = (K - K_0)/(1 - K_0) \tag{11}$$

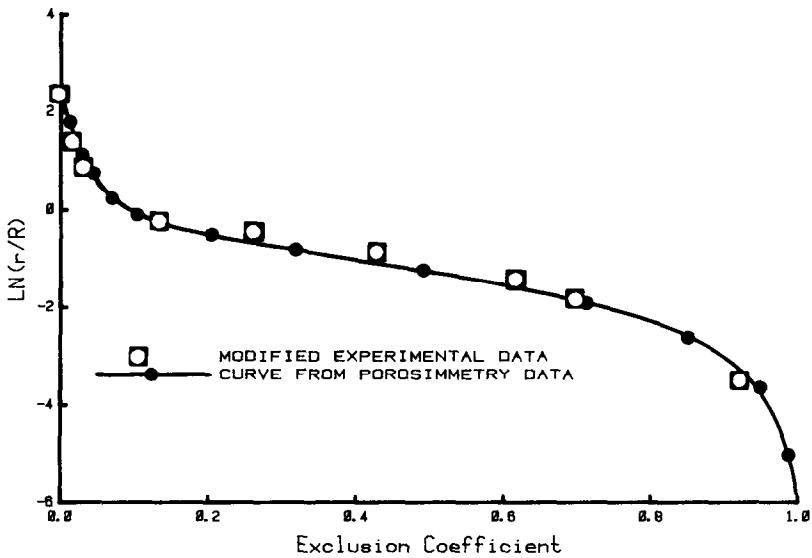

Fig. 14. Comparison of experimental data for Hypersil with exclusion curve calculated from pore-size distribution curve of Fig. 13.

In the case of Hypersil (Fig. 1) the largest molecular radius was 700 Å and the most convenient cut-off point on the calibration curve (Fig. 12) was at $R = 4000$ Å, a value of R just below that at which the interparticle pores start contributing to the pore volume. Accordingly, the pore size distribution curve used is that given in Fig. 13; some smoothing of the experimental data has been introduced. The pore volume was divided into convenient segments, as shown in this figure: the proportion given beside each segment is the value used for $f(R)$ in eqn. 9. K_0 for the 700 Å radius polystyrene was found to be 0.013, and eqn. 11 was used to obtain new K values such that K for this species was exactly zero. The theoretical exclusion curve so calculated for Hypersil is shown in Fig. 14. The agreement between experiment and theory is extraordinarily good and well within experimental error.

It is important to note that *no adjustable parameters* have been used in making the correlation between experiment and theory. The experimental exclusion data rely only upon direct measurement of retention times, and the use of the well-established eqn. 7 relating the radii of random coil polymeric polystyrenes to their molecular weights; the theoretical curve is calculated using totally independent porosimetry data obtained by an independent laboratory (Coulter Electronics, Dunstable, U.K.).

The excellence of the fit between theory and practice establishes again that the exclusion phenomenon can be quantitatively explained on a purely steric basis and, of more practical importance, that the exclusion curve for elution of spherical polymer molecules from non-adsorbing matrix can be calculated from mercury porosimetry data.

DETERMINATION OF PORE-SIZE DISTRIBUTION FROM AN EXPERIMENTAL EXCLUSION CURVE

It is fairly obvious that, if a dependence of K upon r can be established by experiment for any material, then it should be possible to deduce the form of the pore-size distribution curve by inversion of eqn. 10. Curves, such as those shown in Figs. 12 and 13, are, of course, cumulative pore-size distribution curves and are related to the differential pore-size distribution function $f'(R)$ by eqn. 12.

$$g(R) = 1 - \int_0^R f'(r)\,dr \tag{12}$$

Using eqn. 10, it may be shown (see Appendix) that $f'(R)$ is given by eqn. 13

$$f'(R) = -\frac{R^2}{2}\left(\frac{d^3K}{dr^3}\right)_{r=R} \tag{13}$$

$g(R)$, obtained by integration, may then be expressed in either of two forms given by eqns. 14 and 15 (see Appendix).

$$g(R) = K - R\left(\frac{dK}{dr}\right)_{r=R} + \frac{R^2}{2}\left(\frac{d^2K}{dr^2}\right)_{r=R} \tag{14}$$

$$g(R) = K - \frac{3}{2}\left(\frac{dK}{d \ln r}\right)_{r=R} + \left(\frac{1}{2}\frac{d^2K}{d\,(\ln r)^2}\right)_{r=R} \quad (15)$$

The second of these equations is the more useful, since it makes direct use of the usual plot of ln r against K. In order to exploit eqn. 15 to maximum advantage it is desirable to fit the experimental exclusion data to a smooth analytical expression, such as a polynomial, so that explicit expressions can then be obtained for the differentials. Alternatively, it is possible to differentiate the smoothed exclusion curve graphically and so derive the cumulative pore-size distribution curve. In Fig. 13 the graphical procedure has been applied to derive the points marked by circles. Agreement with the original, smoothed experimental curve is seen to be excellent, even with such a simple calculation procedure.

The application of this method to the SEC calibration curves of Fig. 1 is shown in Fig. 15. For this purpose the exclusion curves have been redrawn as plots of K against ln r, (Fig. 15A). These curves are differentiated graphically to give first and second derivatives functions of ln r. Finally $g(R)$ is obtained using eqn. 15. The resulting cumulative pore-size distribution (PSD) curves are shown in Fig. 15B.

These curves show a number of interesting features. Firstly, the PSD curves

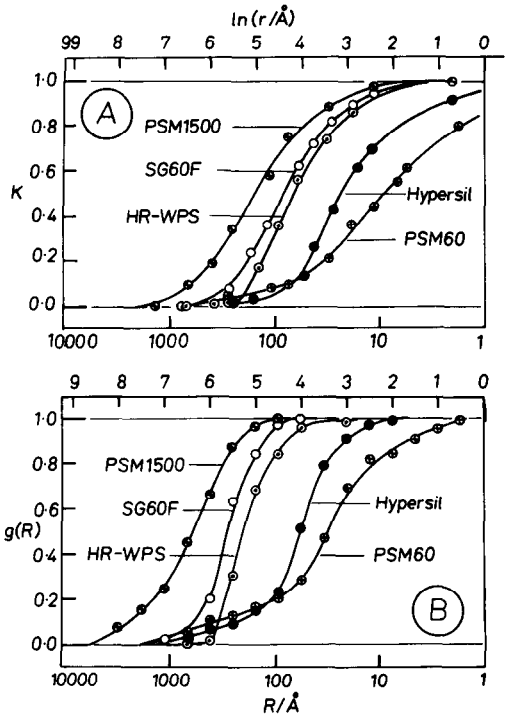

Fig. 15. Pore-size distribution curves derived from size-exclusion calibration curves. (A) Experimental SEC data plotted as dependence of K upon ln r (data of Fig. 1). (B) Calculated pore-size distribution curve, obtained by graphical differentiation of SEC curves and application of eqn. 15. Points are individually calculated values.

show a much steeper dependence upon pore radius than do the plots of K against ln r. This is as expected, since even a step function PSD (such as that representing a uniform cylinder) gives a sloping dependence of K upon r (Figs. 3 and 4). Secondly, the five materials show significantly different PSD curves. The narrowest PSD is exhibited by the new WLCU experimental wide-pore, high-porosity silica gel, which has a PSD curve rather similar to that of the experimental material SG60F, produced by AERE, Harwell, U.K. This latter material was, however, extremely fragile in contrast to the WLCU material. Hypersil has a slightly wider PSD with a significant proportion of pores substantially larger than the mean. The PSM materials, produced by Du Pont technology, have much broader PSD's and the small-pore material PSD60 has a particularly large proportion of both large and small pores. Fig. 1 shows that the newer WLCU material (HR-WPS) has a relatively large value of V_p/V_0, which is desirable for SEC where peak capacity is a strong function of this ratio, whereas the PSM materials of relatively low particle porosity (50–60%) have a rather small V_p/V_0 ratio.

It is evident that the *pore-size distributions may now be simply determined from experimental exclusion curves of the spherical polymer molecules eluted from SEC materials.*

The above results may usefully be discussed in relation to a previous proposal by Halász and co-workers[14,19,20] for determining pore-size distributions from exclusion data. The method proposed by Halász uses the exclusion curve directly as a measure of the cumulative pore size distribution curve. He states, for example (ref. 14), "determination of the elution volumes of two standard samples with molecular weights M_1 and M_2 (where $M_1 < M_2$) gives the relationship $\Delta V = V_{e,1} - V_{e,2}$. ΔV is the volume of pores within the column that have a diameter greater than φ_1 and smaller than φ_2". This is equivalent to the assumption that the exclusion curve for a matrix of uniform cylindrical pores is a horizontal straight line, that is, that there is a sudden change from total exclusion when $r > R$ to total permeation when $r < R$. Regrettably, this assumption is incorrect, as can be seen from Figs. 2 and 3 and, in general, from the introductory section of this paper and other similar treatments[3]. The discrepancy between the pore-size distribution curves obtained from the two theories is well illustrated by Fig. 15. According to the proposal of Halász, Fig. 15A would represent the PSD curves for the materials in question. His method has two serious defects in practice: (1) the true pore-size distribution curve lies at considerably higher R values than does the (K,r) curve; (2) the true pore-size distribution curve shows a much sharper transition from zero to unity than does the (K,r) curve. In order to overcome the first defect, Halàsz[14] was forced to "assign pore sizes by trial-and-error to the standards of the calibration series, in such a way that the maxima of the pore-size distribution curves, as measured by exclusion chromatography, agreed with the values obtained by classical measurements". In order to do this "the pore diameter ø of a solid assigned by us to a standard polystyrene of molecular weight, $\bar{M}_w$, is 2.5 times as large as the coil diameter ø of molecules of the same polystyrene". It may be seen from Fig. 15 that shifting the (K,r) curves about 1.1 ln units to higher r values would in fact, make their inflection points more or less coincide with those of the pore size distribution curves, that is to fit the two curves would require r to be increased by a factor of about 3 rather than 2.5, but, of course, the slopes of the curves would still be wrong. It is clear that the difficulties which

were encountered by Halász[14] in applying his theory arose entirely from an incorrect initial assumption*. By using the correct formulation of the exclusion of spherical molecules from cylindrical pores an entirely self-consistent theory of exclusion can be derived, which gives quantitative agreement between experiment and theory without any arbitrary assumptions.

The problem of deriving pore-size distribution curves from measurements in exclusion chromatography may now be considered solved.

CONCLUSIONS

Several models have been found to predict size exclusion calibration curves with high precision. The best of these theoretical models are the random-sized touching sphere model, developed by the authors, and the uniform-sized random-sphere model of Van Krefeld and Van den Hoed. Both models give excellent quantitative fits to experimental data with no adjustable parameters. The main features which a model must possess to give accurate quantitative prediction of SEC calibration curves are:

(1) the model should possess the same porosity as the material being modelled so that there is a realistic relationship between the pore size and the basic structural unit of the model.

(2) the model must exhibit a sufficient range of pore size. This is best achieved by employing building units which themselves have a range of sizes and by assembling them in a non-uniform manner,

(3) to model very wide pores which appear in real materials it may be necessary to introduce arbitrary defects into the model.

In general, these models fit best in the region of low and intermediate molecular weight and least well at high molecular weight. This is almost certainly due to the presence of large pores in real materials, which cannot be satisfactority modelled.

It is shown that SEC calibration curves can also be predicted with remarkable accuracy from mercury porosimetry data, by using a model consisting of an assembly of cylindrical pores having the pore size distribution given experimentally. Inversion of this procedure enables the pore size distribution of a material to be derived from the SEC calibration curve. The method is applied to five representative SEC materials which show significantly different pore-size distributions. The new procedure provides an important new method for determination of pore size distributions in mesoporous materials. A serious error in previously recommended procedures is noted and corrected.

APPENDIX

Derivation of eqns. 9 and 10

K is the fraction of the total pore volume of the matrix which is accessible to

---

* *Note added in proof*: This same error has been included in two recent treatments of the derivation of pore-size distributions from polymer exclusion curves, namely the papers by F. V. Warren, Jr. and B. A. Bidlingmeyer, *Anal. Chem.*, 56 (1984) 950 and by R. D. Hester and P. H. Mitchell, *J. Liq. Chromatogr.*, 7 (1984) 1511.

a molecule of radius r. We assume the matrix to be made up of an array of cylinders. The fraction of the total volume comprising cylinders of radius R is denoted by $f(R)$.

For any group of cylinders of radius R the fraction of volume accessible to a molecule of radius r is given by eqn. 1, namely

$$K = \left(1 - \frac{r}{R}\right)^2; \qquad R \geqslant r \tag{1) (a}$$

The volume of this group of cylinders is $f(R)V$ where V is the total volume of all cylinders. Thus the amount of accessible volume for this group of cylinders is

$$V_{acc} = \left(1 - \frac{r}{R}\right)^2 f(R)V \tag{b}$$

The total accessible volume for all groups of cylinders is

$$V_{acc} = \sum_{R=r}^{\infty} \left(1 - \frac{r}{R}\right)^2 f(R)V \tag{c}$$

The fraction of volume accessible is then

$$K = \frac{V_{acc}}{V} = \sum_{R=r}^{\infty} f(R) \left(1 - \frac{r}{R}\right)^2 \tag{9) (d}$$

Alternatively, if $f'(R)dR$ is the fraction of pore volume contained in pores having radii between R and $R+dR$, eqn. 10 may be derived.

$$K = \frac{V_{acc}}{V} = \int_{r}^{\infty} f'(R) \left(1 - \frac{r}{R}\right)^2 dR \tag{10}$$

It is important to note that K is a function only of r and that the integration limits are from r to infinity, since negative values of $(1 - r/R)$ must not contribute.

Derivation of eqns. 13 and 14

Differentation of eqn. 10 gives

$$\frac{dK}{dr} = -\left[f'(R)\left(1 - \frac{r}{R}\right)^2\right]_{R=r} - \int_{r}^{\infty} \frac{2}{R} f'(R)\left(1 - \frac{r}{R}\right) dR \tag{e}$$

The first term on the right-hand side is zero. Differentiating a second time gives

$$\frac{d^2K}{dr^2} = +\left[\frac{2}{R} f'(R)\left(1 - \frac{r}{R}\right)\right]_{R=r} + \int_{r}^{\infty} \frac{2}{R^2} f'(R)dR \tag{f}$$

Again the first term on the right-hand side is zero. Differentiating a third time gives

$$\frac{d^3K}{dr^3} = -\left[\frac{2}{R^2} f'(R)\right]_{R=r} = -\frac{2}{r^2} f'(r) \qquad (g)$$

or rearranging

$$f'(r) = -\frac{r^2}{2}\left(\frac{d^3K}{dr^3}\right) \qquad (13)\ (h)$$

The cumulative pore size distribution, $g(R)$, is obtained by integration of $f'(R)$ as

$$g(R) = 1 - \int_0^R f'(R)\, dR \qquad (i)$$

$$= 1 + \int_0^R \frac{r^2}{2}\frac{d^3K}{dr^3}\, dr \qquad (j)$$

Integrating by parts and noting that $K = 1$ when $r = 0$ gives finally

$$g(R) = \frac{R^2}{2}\left(\frac{d^2K}{dr^2}\right)_{r=R} - R\left(\frac{dK}{dr}\right)_{r=R} + K \qquad (14)\ (k)$$

In this equation d^2K/dr^2 is always positive while dK/dr is always negative. Thus all three terms contribute in the same direction to $g(R)$.

Since $g(R)$ and K are normally plotted as functions of ln R, it is more useful to express $g(R)$ in the form of eqn. 15.

$$g(R) = \frac{1}{2}\left(\frac{d^2K}{d(\ln r)^2}\right)_{r=R} - \frac{3}{2}\left(\frac{dK}{d\ln r}\right)_{r=R} + K \qquad (15)\ (l)$$

Now, the first term changes sign, being negative at low r and positive at high r. The second term, however, is always negative.

REFERENCES

1 G. J. Kennedy and J. H. Knox, *J. Chromatogr. Sci.*, 10 (1972) 549.
2 J. H. Knox, R. Kaliszan and G. J. Kennedy, *Faraday Symp.*, 15 (1980) 113.
3 W. W. Yau, J. J. Kirkland and D. D. Bly, *Modern Size-Exclusion Chromatography*, Wiley, New York, 1979.
4 J. C. Moore, *J. Polym. Sci.*, A2, (1964) 835.
5 J. Porath and P. Flodin, *Nature (London)*, 183 (1959) 1657.
6 W. W. Yau and P. Malone, *J. Polym. Sci.*, B12 (1974) 277.
7 E. A. Di Marzio and C. M. Guttman, *J. Polym. Sci.*, B7 (1969) 267.

8 C. M. Guttman and E. A. Di Marzio, *Macromolecules*, 3 (1970) 681.
9 J. C. Giddings, E. Kucera, C. P. Russel and M. N. Myers, *J. Phys. Chem.*, 72 (1968) 4397.
10 E. F. Casassa, *J. Phys. Chem.*, 75 (1971) 3929.
11 J. H. Knox and F. McLennan, *J. Chromatogr.*, 185 (1979) 289.
12 W. Haller, *J. Chem. Phys.*, 42 (1965) 686.
13 M. E. Van Krefeld and N. Van den Hoed, *J. Chromatogr.*, 83 (1973) 111.
14 I. Halász and K. Martin, *Angew. Chem. Int. Ed. Engl.*, 17 (1978) 901.
15 D. J. Adams and A. J. Matheson, *J. Chem. Phys.*, 56 (1972) 1989.
16 W. M. Vischer and M. Bolsterli, *Nature (London)*, 239 (1972) 504.
17 H. P. Scott, *Ph. D. Thesis*, University of Edinburgh, Edinburgh, 1983.
18 A. J. de Vries, M. Le Page, R. Beau and C. L. Guilleman, *Anal. Chem.*, 39 (1967) 935.
19 R. Niklov, W. Werner and I. Halász, *J. Chromatogr. Sci.*, 18 (1980) 207.
20 T. Crispin and I. Halász, *J. Chromatogr.*, 239 (1982) 351.